Modifying Montmorillonite Clay via Silane Grafting and Interfacial Polycondensation for Melt Compounding of Nylon-66 Nanocomposite

Hamid Salehi-Mobarakeh, Ali Yadegari, Fahimeh Khakzad-Esfahlan, Alireza Mahdavian

Department of Polymer Science, Faculty of Science, Iran Polymer and Petrochemical Institute, Tehran, Iran

Received 3 May 2011; accepted 29 June 2011
DOI 10.1002/app.35159
Published online 18 October 2011 in Wiley Online Library (wileyonlinelibrary.com).

ABSTRACT: A trifunctional organo alkoxysilane (3-aminopropyl)triethoxysilane (γ-APS) has been used as reagent for the chemical modification of montmorillonite clay. Silane grafting was taken place in dry and hydrolyzing conditions. Silane grafted and pristine clay took part in interfacial polycondensation process to deposit a layer of nylon-66 onto the clay lamellae and therefore, enhance their affinity with nylon-66 matrix. Evidence of presence of grafted silane molecules and deposition of nylon-66 on clay particles were provided by Fourier transform-infrared, thermogravimetric analysis (TGA), and X-ray diffraction (XRD). Such modified clays and pristine clays were melt compounded with nylon-66. The structures of the resulting nylon composites were characterized using XRD and transmission electron microscopy and the results showed presence of both intercalation and exfoliation. TGA thermograms of nanocomposites indicated improved thermal stability upon the incorporation of silane grafted montmorillonite. Furthermore, differential scanning calorimetry scans showed that silane modified clays promoted crystallization in nanocomposites. Increase of storage modulus and depression of tan δ peak in nanocomposites in dynamical mechanical thermal analysis were observed. The rheological properties of nylon-66 and nanocomposites were also evaluated and differences in values of complex viscosity of samples were noticed. © 2011 Wiley Periodicals, Inc. J Appl Polym Sci 124: 1501–1510, 2012

Key words: nylon; nanocomposites; modification; clay; polycondensation

INTRODUCTION

Polymer-layered silicate nanocomposites have received both academic and industrial interest because they exhibit significant improvement in properties at very low percentage of filler relative to conventional composites. Study of these materials came into vogue with the work initiated by the Toyota research team.[1,2] They investigated the ability of organically modified montmorillonite to be swollen by the ε-caprolactam monomer and arranging *in situ* intercalative polymerization to achieve nylon-6-based nanocomposites.[3,4]

Under natural condition, the individual sheets of montmorillonite stack together via the Van der Waals forces to form macroscopic clay particles called tactoids.[5] Due to the intrinsic polarity, inorganic clays are incompatible with organic phases and, therefore, it is essential to modify their surfaces to make them organophillic and increase their gallery height.[6,7] The mostly used modification approach is the ion exchange reaction with alkyl ammonium surfactants. The onset temperature of decomposition of these modified clays is approximately 180°C. If the processing temperature is higher than the thermal stability of the organic treatment on the clay, decomposition will happen.[8]

An alternative modification method involves direct grafting reaction to form covalent bonds. Presence of silanol groups on the edge of clay due to the broken edge and crystalline defects, enables grafting of alkoxyl silanes to the clay edge via condensation with these silanol groups. Furthermore, the interlayer grafting can happen within the clay gallery and leads to prominent increase of the clay basal spacing. Compared with the ion-exchanged clays that ammonium molecules are physically adsorbed, the covalently modified clays exhibit improved thermal stability.[9–12]

It has been reported that sylilation reaction and the interlayer structure of grafted products depend on the kind of used clay materials.[13] The influence of dispersing medium on grafting of organosilane onto the montmorillonite surface has been studied by Shanmugharaj et al.[14] They concluded that the surface energy of used solvent plays an important role on grafting reaction. Herrera et al.[9,15] inspected effects of silane functionality on the sylilation of laponite. Another method for silane grafting has been reported in which sylilation is carried out by

Correspondence to: H. Salehi-Mobarakeh (h.salehi@ippi.ac.ir).

exposing montmorillonite to saturated vapor from refluxing silane.[16] Dean et al.[17] developed urethane acrylate nanocomposite using silane grafted montmorillonite. The organosilanes which were used contained acrylate functionality which could react with the acrylate groups in the urethane acrylate matrix. Preparation of polycarbonate, unsaturated polyester, polyethylene, epoxy, poly(ethylene terephthalate), poly(butylene terephthalate) nanocomposites based on silane grafted montmorillonite has also been reported.[11,18–23]

Nylon-66 or poly(hexamethylene diamine-*co*-adipic acid), first prepared by Carothers in 1936, is one of the two principal polyamides, the other is nylon-6, in commercial production.[24] Despite the fact that nylon-66 is an important engineering polymer, it received little attention to prepare clay nanocomposites. To our knowledge, silane grafted montmorillonite has not been utilized in nylon-66 nanocomposites. In this work, sylilation of clay lamellae is followed by interfacial polycondensation (IPC) of diamine and diacid chloride to deposit a layer of nylon-66 onto the clay lamellae, and thus being more compatible with nylon matrix, in addition to improved thermal stability due to silane agents. So far, preparation of nylon-66 nanocomposites using IPC has been reported, but all of them have organized IPC process to provide final nanocomposite product.[25–27] It is obvious that this procedure is not commercially reasonable, because of high costs of the IPC process.

This work presents employing of IPC to modify pristine and silane grafted montmorillonite for melt compounding of nylon-66 nanocomposite, and thus more compatibility and thermal stability of the hybrid product.

EXPERIMENTAL

Materials

The nylon-66 used in this study was obtained from DuPont Company (Zytel). Sodium montmorillonite (Na-MMT) was Kunipia-F with cation exchange capacity of 119 meq/100 g, was kindly supplied by Kunimine Industry, Japan. The trifunctional sylilating agent (3-aminopropyl)triethoxysilane (γ-APS) used for the chemical modification of montmorillonite, was purchased from Aldrich Chemical Company; 1,6-diaminohexane (HMDA) and adipoyl chloride (AdCl) from Aldrich (Germany), were used in IPC to further modification of clay lamellae. Triethylamine (Merck, Germany) was added as a scavenger for the byproduct in IPC process. Solvents used in this work were toluene (Acros Organics), distilled water, and pure ethanol.

Modification of montmorillonite

Silane grafting

Two grams of Na-MMT was dispersed in 75 mL of toluene, and 1 mL of γ-APS, corresponding to more than 6 meq of silane per gram of clay, was added into the reaction flask and experienced sonication using an ultrasonic probe homogenizer (Bandelin Sonoplus, Germany), for 30 min at a power of 65%. It was then washed with toluene repeatedly, dried preliminary, ground in a mortar, and then dried at 50°C under vacuum condition before processing or analysis. Another silane grafting process was performed by following the sonication step in water/ethanol (20/80 by volume) resulting in a three-component solution of toluene–water–ethanol. Ethanol content provides a homogenous mixture of immiscible ingredients of water and toluene. It was mixed vigorously using a magnetic stirrer at 80°C for 3 h. The reaction product was extensively washed with ethanol and water, ground, and dried at 50°C in a vacuum oven. Samples were designated as TS-MMT (silane grafted MMT in toluene) and HS-MMT (silane grafted MMT in toluene which is followed by mixing in water–ethanol solution).

Interfacial polycondensation

In this step Na-MMT, TS-MMT, and HS-MMT entered in interfacial polycondensation (IPC) process. Each clay was dispersed in aqueous phase (2 g clay in 200 mL water), and consequently 0.21 g HMDA and 0.36 g triethylamine were introduced into the suspension. With the addition of HMDA, flocculation of clay lamellae takes place, which is the result of destruction of double layer keeping particles in suspension.[28] Then 200 mL toluene (organic phase) contained 0.32 g AdCl, poured into the aqueous phase, while the mixture is blended at 16,000 rpm by a disperser (Ultra-Turrax, IKA, Germany). IPC process lasted for 7 min. The products were washed with ethanol and water, and after grinding, dried in a vacuum oven at 50°C. Na-MMT, TS-MMT, and HS-MMT that underwent IPC process, designated as INa-MMT, ITS-MMT, and IHS-MMT, respectively.

Melt compounding

Nanocomposites were prepared by melt blending Na-MMT, INa-MMT, ITS-MMT, and IHS-MMT with nylon-66 using a Brabender mixer, at 80 rpm for 6 min at 270°C. Before blending, all MMT samples and nylon-66 were dry mixed and dried at 80°C for 24 h under vacuum condition. The MMT content in each sample was 5 wt %. Since the amount of MMT

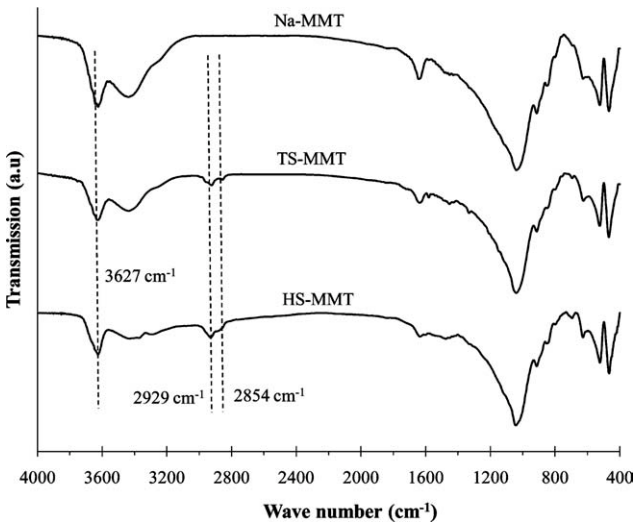

Figure 1 FT-IR spectra of Na-MMT and silane grafted montmorillonites.

in all samples was the same, henceforth, the sample compositions will not be mentioned in the text.

Characterization

The chemical modification of the clay was investigated using a Bruker (Equinox 55) Fourier transform-infrared spectrometer (FT-IR), on powder-pressed KBr pellets. The spectra were taken over the spectral range 400 to 4000 cm^{-1} with a resolution of 4 cm^{-1}.

X-ray powder diffraction (XRD) patterns were obtained from a Philips Analytical diffractometer, using Cu-Kα radiation ($\lambda = 0.154$ nm), operating at 40 kV and 40 mA.

Thermogravimetric analysis (TGA) was performed using a TGA-PL instrument. The clays and the resulting nanocomposites were heated at rates of 20 and 10°C/min, respectively, under a nitrogen flow.

Differential scanning calorimetry (DSC) was performed with Polymer Laboratories (PL-DSC), the samples were weighed and heated from 30 to 300°C at a heating rate of 10°C/min under nitrogen atmosphere. The samples were held at 300°C for 5 min to eliminate previous history, and then cooling and second heating were performed at a rate of 10°C/min.

Dynamic mechanical properties were evaluated on a Dynamic Mechanical Analyzer (Tritec 2000 DMA). The dual cantilever bending mode was used in a temperature range from 0 to 250°C. The heating rate and frequency were 5°C/min and 1 Hz, respectively.

Rheological measurements were obtained in dynamic mode of shearing on a Modular Compact Rheometer, Anton Paar, with a parallel plate fixture (25 mm diameter). The frequency range was set at 0.01 to 600 rad/s and the applied strain was 10% at 270°C.

Transmission electron microscopy (TEM) was carried out using a Zeiss EM10C transmission electron microscope operated at 80 keV. Cross-sections of the nanocomposites were obtained by slicing the sample into thin films of about 70 to 100 nm thickness.

RESULTS AND DISCUSSION

Modification of montmorillonite

Silane grafting

The modified and sodium montmorillonite clays were characterized using FT-IR, XRD, and TGA to evaluate silane grafting and insertion of nylon layer on clay platelets in IPC process. Figure 1 shows the FT-IR spectra of Na-MMT and the silane grafted montmorillonites. The spectra show the peak at 3627 cm^{-1} corresponding to stretching vibration of the surface hydroxyl groups that are bonded to the aluminum and magnesium in montmorillonite. After silane grafting reaction, intensity of this band decreases. This decrease is more evident for HS-MMT, indicating more silane molecules participated in the grafting reaction. New peaks at 2929 cm^{-1} with a small hump at 2854 cm^{-1} referring to —CH asymmetric and symmetric stretching of CH_2 groups are observed in TS-MMT and HS-MMT spectra, which indicates the presence of γ-APS in modified clays.

The XRD patterns of the silane grafted montmorillonites and pristine clay are shown in Figure 2. Na-MMT has a characteristic diffraction peak at $2\theta = 9.05°$ attributed to basal spacing (d_{001}) of 9.76 Å. It can be seen that basal spacing for TS-MMT is 9.73 Å which is close to d_{001} of Na-MMT. Despite utilizing ultrasonic probe homogenizer, hydrophilicity of Na-MMT prevents dispersing of clay lamellae in toluene, and during grafting process, silane molecules cannot diffuse in the gallery of clays, and basal

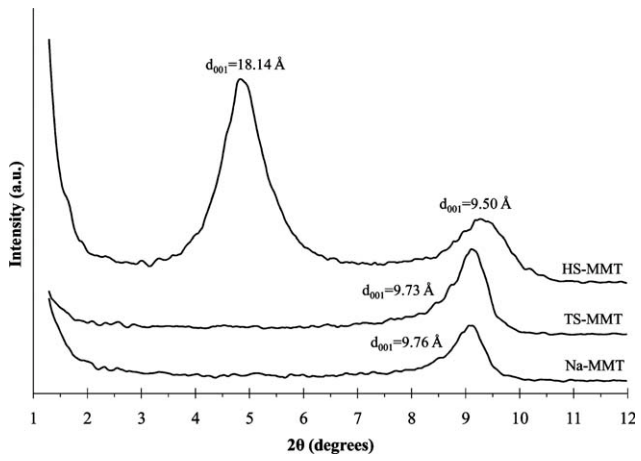

Figure 2 XRD patterns for Na-MMT and silane grafted montmorillonites.

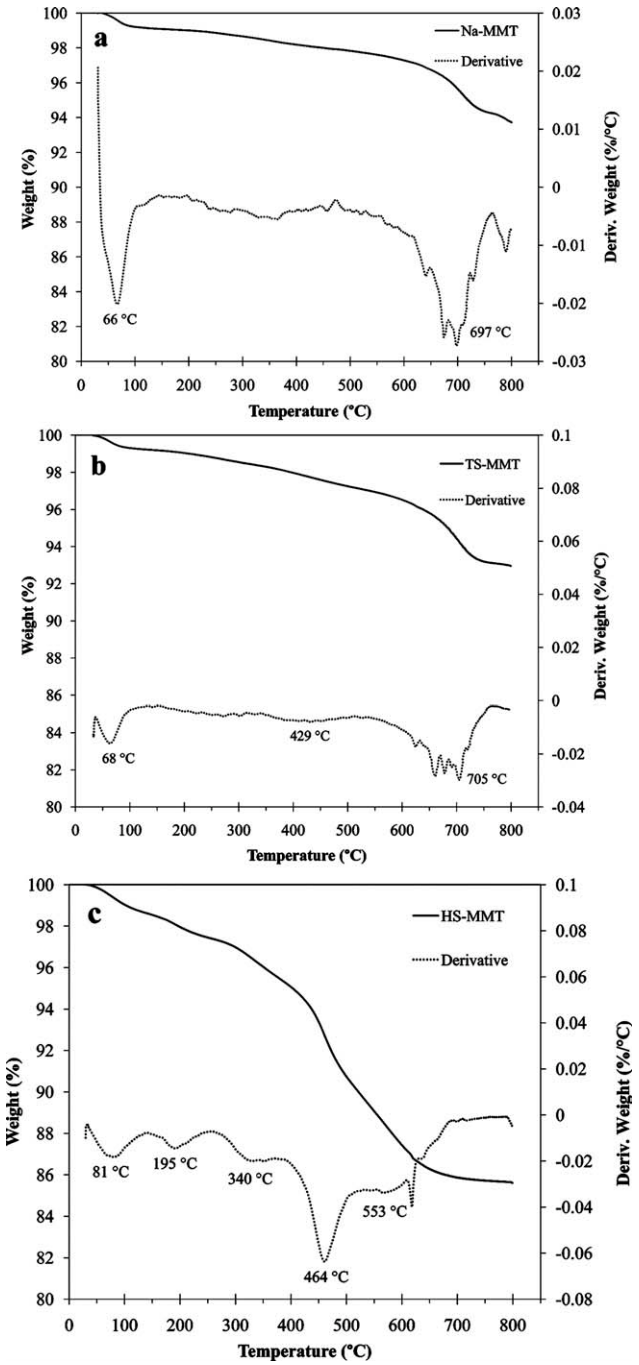

Figure 3 TGA thermograms of clays before and after silane grafting, (a) Na-MMT, (b) TS-MMT, and (c) HS-MMT.

spacing remains constant. For the HS-MMT two peaks are observed at $2\theta = 9.29°$ and 4.86° corresponding to 9.50 Å and 18.14 Å, respectively. Presence of water in the reaction favors the exfoliation of clay platelets, and the amount of grafted silanes increases the d_{001} spacing of clay by 8.38 Å.

Figure 3 displays the TGA thermograms of clays before and after grafting of the silane molecules. The DTG curve of Na-MMT [Fig. 3(a)] shows two peaks at 66°C and 697°C, attributing to loss of the physically adsorbed water and irreversible dehydroxylation of clay, respectively. For TS-MMT, in addition to the peaks due to loss of surface water (68°C) and dehydroxylation of clay (705°C), a weak broad peak is observed at 429°C [Fig. 3(b)] corresponding to loss of small amount of grafted silane to the edge of clays. As was seen in the XRD pattern of TS-MMT, where there is no increase in the gallery height, silane molecules cannot reach the clay interlayer, and condensation reaction takes place at the clay edges. The DTG curve for HS-MMT [Fig. 3(c)] displays five peaks at 81, 195, 340, 464, and 535°C, respectively. The peak at 81°C is attributed to the vaporization of free water, while the peak at 195°C is possibly corresponding to the loss of adsorbed γ-APS molecules. Weight loss at 340°C refers to intercalated silane between clay platelets. In addition, the peaks at 464 and 535°C are due to decomposition of chemically grafted silane with the clay lamellae and in the clay interlayer, respectively. There is no any evident peak for dehydroxylation of HS-MMT. Lack of hydroxyl weight loss in HS-MMT, may present that hydroxyl groups were consumed in grafting reaction.[12] The amount of grafted silane in TS-MMT is about 2.5 wt %, while this value for HS-MMT is about 10.5 wt %.

These results indicate that grafting yield is strongly affected by the used solvent. Na-MMT has a tendency to pile up into tactoids when suspended in nonpolar liquids such as toluene. Therefore, in the case of TS-MMT, dispersion of clay lamellae cannot occur and silane agents have little chance to reach the interlayer of clay, and grafted amount is low. Furthermore, presence of water, in addition to dispersion of clay, leads to hydrolyzing of silane molecules and condensation reaction with hydroxyl groups of clay takes place.

Interfacial polycondensation

FT-IR spectra of montmorillonites which took part in interfacial polycondencation process, INa-MMT, ITS-MMT, and IHS-MMT, are shown in the Figure 4. Presence of nylon-66 on the clay platelets are observed via peaks at 1639 and 1540 cm^{-1} corresponding to amide I and amide II, respectively,.[29] The N—H stretching vibration at 3311 cm^{-1} is apparent after IPC process. The peak at 2938 cm^{-1} referring to stretching vibration of C—H band, is stronger for ITS-MMT and IHS-MMT comparing with TS-MMT and HS-MMT shown in Figure 1, indicating the presence of methylene groups of nylon chains on the clay.

The X-ray diffractograms of the INa-MMT, ITS-MMT, and IHS-MMT are presented in Figure 5. The pattern for the INa-MMT reveals that the peak shifted toward smaller angles compared with Na-MMT ($d_{001} = 9.76$ Å), and IPC process increased the

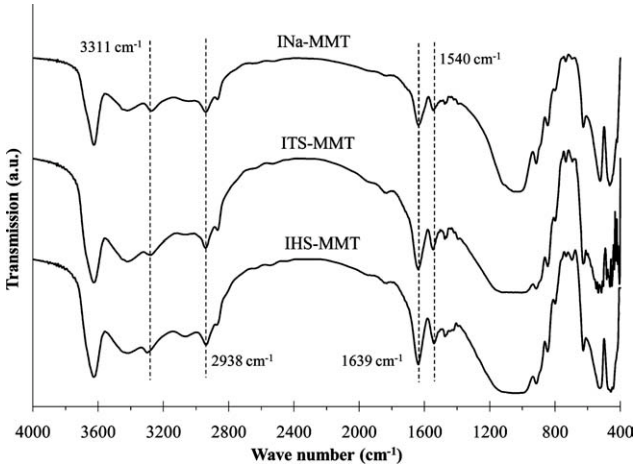

Figure 4 FT-IR spectra of INa-MMT, ITS-MMT and IHS-MMT.

basal spacing of INa-MMT to 13.34 Å, showing that resulted nylon chains diffused through the interlayer of clay platelets. The same behavior is observed for ITS-MMT, and its basal spacing increased to 13.33 Å. As previously mentioned, silane content of TS-MMT is low and its gallery height is close to that of Na-MMT, therefore, similarity in the resultant IPC products is acceptable. There is a peak at $2\theta = 6.56^\circ$ referring to d_{001} spacing of 13.47 Å in the IHS-MMT pattern. In this case, the higher basal spacing in the HS-MMT, 18.14 Å, reduced and the initial basal spacing of 9.50 Å increased to 13.47 Å with IPC process. The most likely explanation for the reduction in basal spacing is that some intercalated silane molecules are present between the clay nanosheets which are not chemically bonded and, therefore, during IPC process can be withdrawn from nanosheets and the overall *d*-spacing reduces to 13.47 Å.

Thermal degradation behavior of pristine and modified clays are shown in Figure 6. As can be evaluated in the Figure 6, the amount of deposited nylon on the INa-MMT is 11.1 wt %, while this

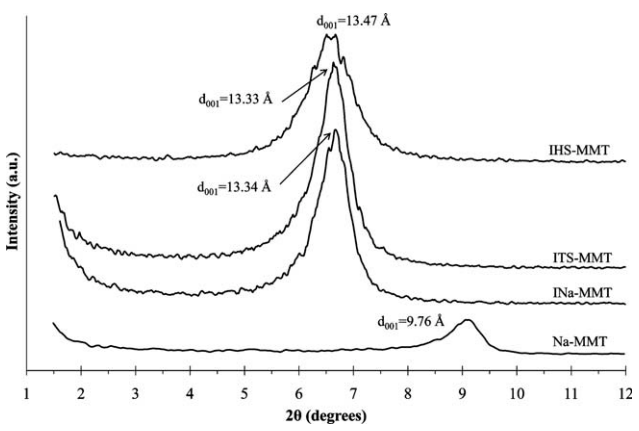

Figure 5 X-ray diffractograms of the Na-MMT, INa-MMT, ITS-MMT, and IHS-MMT.

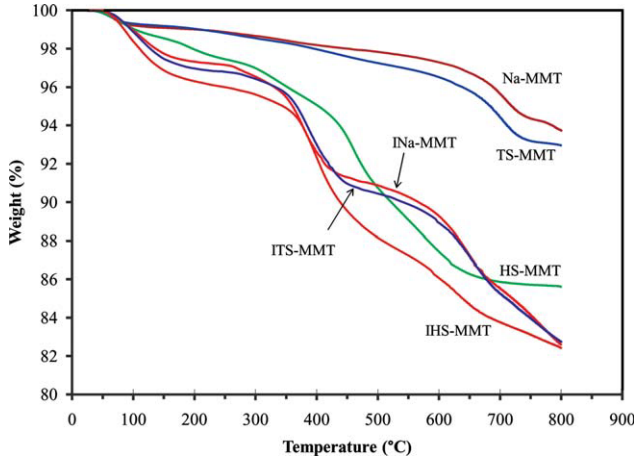

Figure 6 Thermal degradation behavior of pristine and modified montmorillonites. [Color figure can be viewed in the online issue, which is available at wileyonlinelibrary.com.]

value for the ITS-MMT is 10.2 wt %. According to previous results in the silane grafting section, it is expected that nylon content in INa-MMT and ITS-MMT to be close together. The nylon amount in the IHS-MMT is 3.2 wt %. This low value is in accordance with the results obtained by XRD measurements showing that HS-MMT cannot take part in IPC perfectly due to greater grafted silane and thus more hydrophobicity of HS-MMT, therefore, the deposited nylon on clay platelets is in small amount comparing with the two other clays.

Melt compounded nylon-66 nanocomposites

XRD

Figure 7 compares X-ray diffraction patterns for the neat nylon-66 and its nanocomposites containing 5 wt % MMT. The pattern for the nylon-66 has no any characteristic peak in this 2θ range. Nanocomposite

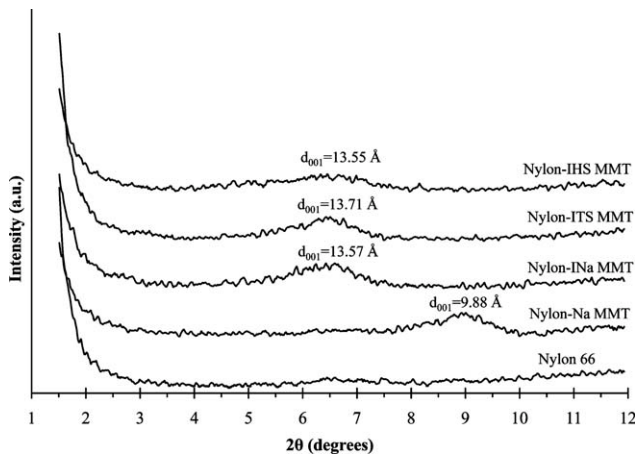

Figure 7 XRD patterns of nylon-66 and nylon nanocomposites.

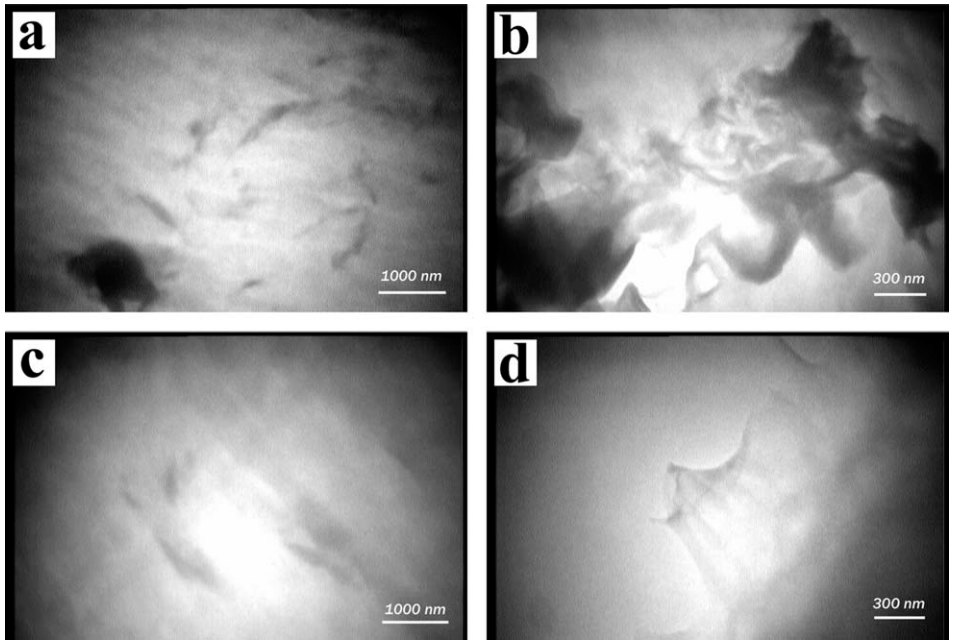

Figure 8 TEM photomicrographs of nylon-66 nanocomposites based on the montmorillonites (a) Na-MMT, low magnification; (b) Na-MMT, high magnification; (c) INa-MMT, low magnification; (d) INa-MMT, high magnification.

including Na-MMT reveals a peak at $2\theta = 8.93°$ indicating the basal spacing of 9.88 Å. For the nanocomposites consisting modified montmorillonites, weak broad peaks are seen. Basal spacing increased slightly for these nanocomposites comparing with their corresponding modified clays. According to Figure 7, basal spacing for nanocomposites based on INa-MMT, ITS-MMT, and IHS-MMT are 13.57, 13.71, and 13.55 Å, respectively. These weak broad peaks disclose that an intermediate organization can exist presenting both intercalation and exfoliation.

Transmission electron microscopy

Figure 8 displays representative transmission electron microscopy (TEM) images of nylon/Na-MMT and INa-MMT nanocomposites. The TEM micrograph of Figure 8(a,b) show that the Na-MMT particles preserved their agglomerated structure. This is in accordance with the result obtained from XRD pattern for Na-MMT nanocomposite which presented a characteristic profile of nanoclay. As it was expected large tactoids of Na-MMT are clearly visible. The INa-MMT nanocomposite showed better dispersion [Fig. 8(c,d)]. It is observed that nanoclay platelets have been delaminated and are more dispersed in the polymer matrix.

Thermogravimetric analysis

Thermal degradation temperature of nylon and its nanocomposites was determined by thermogravimetric analysis. The thermogravimetric analysis (TGA) and DTG thermograms in nitrogen atmosphere are shown in Figure 9(a,b), respectively. In the case of nylon-66, the degradation starts at 337°C, while this value is larger for nylon nanocomposites. The onset temperature of degradation for Na-MMT, INa-MMT, ITS-MMT, and IHS-MMT nylon nanocomposites are 346, 345, 341, and 343°C, respectively. Presence of clay in nylon matrix enhances thermal stability up from 4 to 9°C. The peak of the DTG curves indicates the temperature corresponding to maximum degradation (T_{max}). The T_{onset} and T_{max} of neat nylon and its nanocomposites are given in Table I. As it can be seen, presence of clay and its various treatments have a substantial influence on the thermal stability of nylon due to maximum degradation temperature. A significant increase in T_{max} was observed for IHS-MMT nanocomposite indicating an increase in thermal stability of nylon by 37°C. It is completely in agreement with what is expected from covalently bonded silane molecules in IHS-MMT for improving thermal stability upon the incorporation of silane grafted montmorillonite in nylon matrix.

Differential Scanning Calorimetry

The nonisothermal crystallization exothermal curves of nylon-66 and nylon nanocomposites are depicted in Figure 10. The crystallization temperature, T_c, is about 234.2°C for nylon-66. The addition of Na-MMT into nylon-66 did not change the crystallization temperature, but raised the amount of crystallinity with regards to increased enthalpy of crystallization (Table II). The ratio of heat of fusion

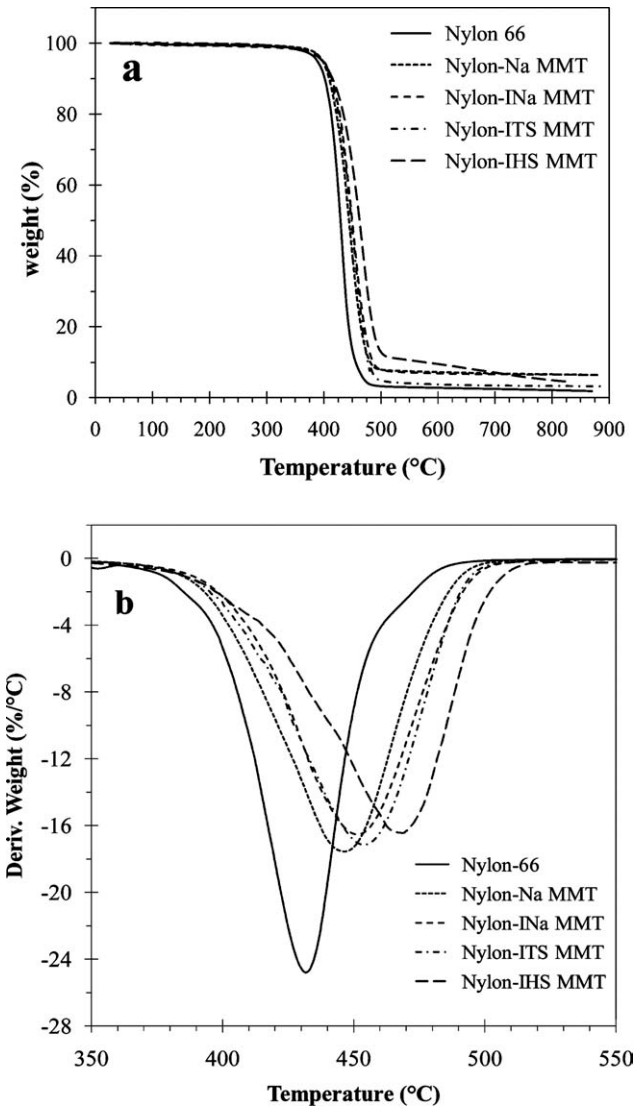

Figure 9 (a) TGA thermograms of nylon-66 and its nanocomposites. (b) Derivative thermograms.

of the sample (ΔH_f) to the heat of fusion of purely crystalline form of nylon-66 (ΔH_f°) was calculated as the percent crystallinity. The ΔH_f° value for nylon-66 matrix was taken as 195.9 J/g.[30] The Na-MMT particles promote the crystallization possibly due to nucleation effect. In the case of INa-MMT, crystallization temperature and enthalpy of crystallization remained similar to that of neat nylon, but in comparison with Na-MMT, its crystallinity decreased. Better dispersion of INa-MMT in the nylon matrix imposed a confinement effect on polymer chain diffusion and crystal growth.[31] Therefore, outcome of nucleation effect and confinement of polymer chains leads to similarity in crystallization temperature and crystallinity of INa-MMT nanocomposite and pristine nylon. Furthermore, lower crystallinity of INa-MMT comparing with Na-MMT nanocomposite can be attributed to the higher viscosity of INa-MMT system, it will be discussed later in this article, which may reduce rate of crystallization. For the silane grafted clays, ITS-MMT and IHS-MMT, the crystallization peak shifted toward higher T_c, which could be ascribed to the effects of silane grafted clays as an efficient nucleating agent to facilitate nylon-66 crystallization. The phenomenon observed here may be attributed to the presence of interactive surfaces that are capable of immobilizing chains in conformations that are more favorable for crystallization,[32] due to possible reactions of carboxyl end groups of nylon-66 with amino group of γ-APS. Therefore, the percent crystallinity of silane grafted clay nanocomposites is higher than other namocomposites and neat nylon, as it can be seen in the Table II.

TABLE I
Effect of Clay Treatment on Degradation Temperatures of Nylon-66 Nanocomposites

Sample	T_{onset} (°C)	T_{max} (°C)
Nylon-66	337	430
Nylon-Na MMT	346	446
Nylon-INa MMT	345	450
Nylon-ITS MMT	341	454
Nylon-IHS MMT	343	467

Figure 11 presents second heating curves of DSC scans. All DSC traces show two crystalline melting peaks at T_{m1} and T_{m2}, which is the result of the dependence of the melting point of crystallites on lamellar thickness. T_{m1} is generally attributed to thin lamella formed during cooling and T_{m2} is attributed to the melting of thickened crystals during the heating or annealing process.[31,33] For the neat nylon and Na-MMT and INa-MMT nanocomposites there is no evident change in the melting points. In silane modified clay nanocomposites both T_{m1} and T_{m2}

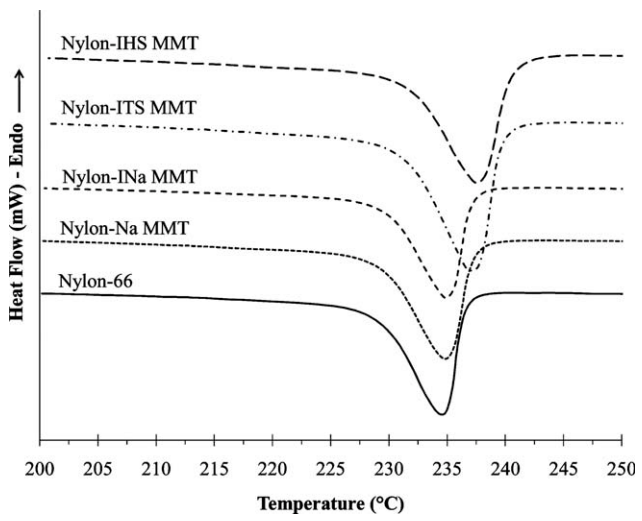

Figure 10 First cooling curves of non-isothermal DSC scans.

TABLE II
DSC Results for Nylon-66 and Nylon Nanocomposites

Sample	T_{m1} (°C)	T_{m2} (°C)	T_c (°C)	ΔH_f (J/g)	Crystallinity (%)
Nylon-66	251.15	260.75	234.19	66.38	33.9
Nylon-Na MMT	251.23	260.79	234.11	73.31	37.4
Nylon-INa MMT	251.4	261.04	234.15	67.44	34.4
Nylon-ITS MMT	254.05	263.57	236.77	75.47	38.5
Nylon-IHS MMT	254.22	263.74	236.73	77.27	39.4

increased which indicates promoting of crystallization. The ratio of heat of fusion of T_{m1} and T_{m2} is approximately constant in all samples, however, it is reported that presence of nanoparticles increases heat of fusion of T_{m1} and decreases that of T_{m2}.[31,34]

Dynamic Mechanical Thermal Analysis

The temperature dependence of storage modulus, E', is shown in Figure 12. It is obvious that introducing of nanoclay into the nylon matrix increased the storage modulus for all temperatures. As it can be seen in Figure 12 modulus enhancement is higher for modified montmorillonites in comparison with Na-MMT. Furthermore, among all nanocomposites, INa-MMT organoclay produced the highest reinforcing effect on nylon. This phenomenon presents that nanoclays and particularly INa-MMT make the stable constrained region in polymer segments.

Figure 13 displays the tan δ data obtained for the neat nylon and nanocomposites. The temperature at the maximum value of tan δ peak is frequently considered as T_g. In the case of Na-MMT nanocomposite, T_g value remained constant, however, for those of organically modified montmorillonites, there is a slight shift in the tan δ peak toward higher temperature. This is in contradiction to results obtained for nylon-6/MMT hybride, in which T_g of nylon-6 decreased.[35] The decrease in the T_g was caused by the alkyl ammonium surfactant in the organic MMT used which was served as a plasticizer during compounding of the organic clay with nylon-6.[36] Therefore, slight increment in T_g value in this study indicates that there is a good affinity between modified clays and nylon-66, and plasticizing effect does not exist. Based on covalently bonded silane molecules and nylon chains utilized as clay modifier, therefore, observed results for T_gs are reasonable.

For each type of montmorillonite, either pristine or modified, it is also observed that the introduction of nanoclays led to a decrease in the height of the tan δ peak, indicating the restricted mobility of polymer chains in the nylon nanocomposites.[37,38] The most height depression in the tan δ peak occurred for INa-MMT nanocomposite which points to the largest amount of constrained region in this hybrid according to a larger contact area between the nanoclay surface and polymer chains.[38]

Rheology

Figure 14 gives logarithmic plots of complex viscosity versus angular frequency for neat nylon-66 and nanocomposites. There are noticeable differences in the low frequency oscillatory data among the

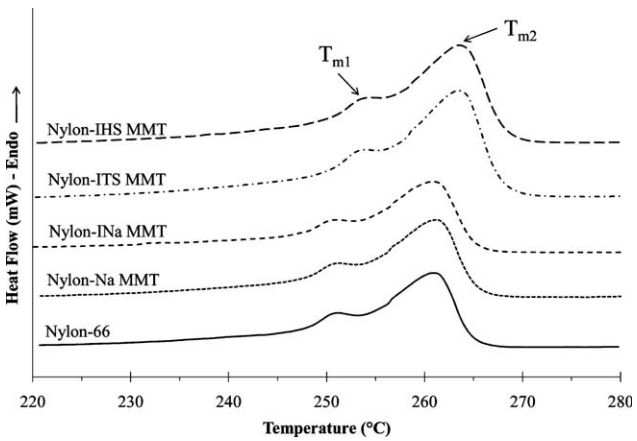

Figure 11 Second heating curves of nonisothermal DSC scans.

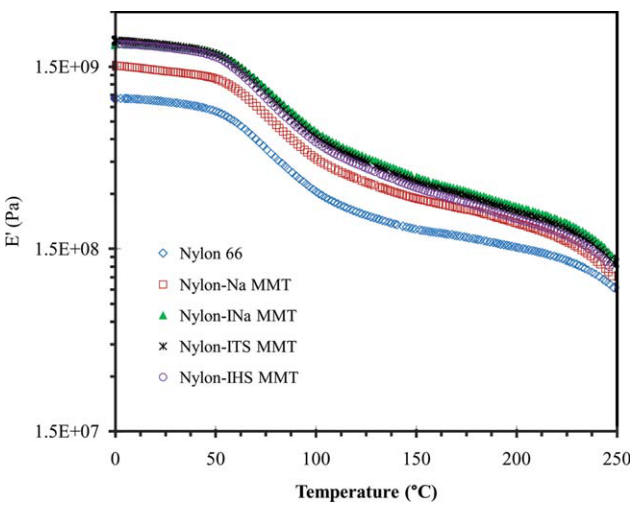

Figure 12 DMTA temperature scans of neat nylon-66 and nanocomposite samples. [Color figure can be viewed in the online issue, which is available at wileyonlinelibrary.com.]

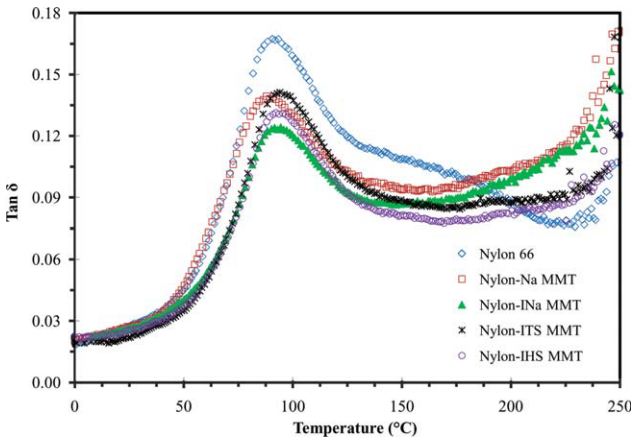

Figure 13 Temperature dependency of tan δ for nylon-66 and its nanocomposites. [Color figure can be viewed in the online issue, which is available at wileyonlinelibrary.com.]

samples. The most Newtonian-like behavior is seen for the pure nylon-66 in the low frequency region. In all nanococomposites, except ITS-MMT, presence of clay increased complex viscosity in low frequency region, in which this increase is more obvious for INa-MMT. In addition, INa-MMT nanocomposite exhibited the strongest shear-thinning behavior over the entire range of angular frequencies. This nanocomposite also produced a weak shear thickening behavior for $\omega < 0.02$ rad/s. The reduction of viscosity due to increment of frequency can be attributed to alignment of silicate layers parallel to the applied shear.[39] In high frequency region the value of the melt viscosity of the nanocomposites was lower than that of pure nylon-66. One possible reason for reduction of melt viscosity in the nanocomposite is slip between the nylon-66 matrix and the exfoliated organoclay platelets during high shear flow.[40] Among

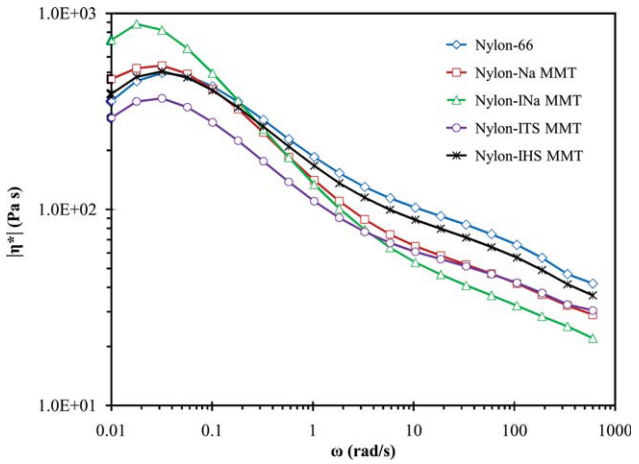

Figure 14 η* curves of nylon-66 and nylon-66/montmorillonite nanocomposites at 270°C. [Color figure can be viewed in the online issue, which is available at wileyonlinelibrary.com.]

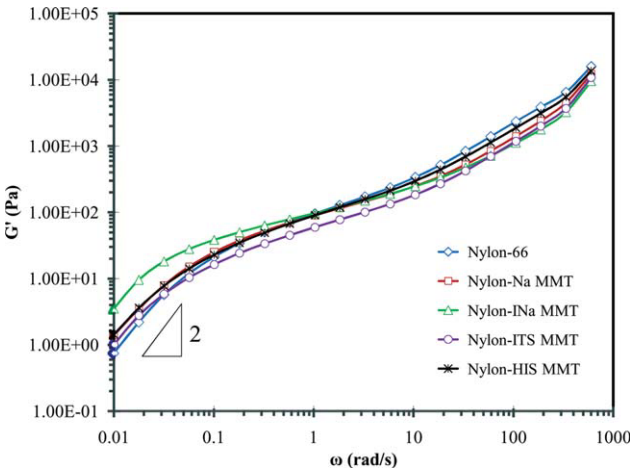

Figure 15 Influence of frequency on shear storage modulus for neat nylon-66 and its nanocomposites. [Color figure can be viewed in the online issue, which is available at wileyonlinelibrary.com.]

various treatments, this slippage is higher in INa-MMT nanocomposite, since better dispersion of INa-MMT in nylon matrix is occurred and, therefore, stronger shear thinning behavior has been observed. Figure 15 presents log G' versus log ω plots at 270°C for nylon-66 and nylon/clay nanocomposites. The plot for nylon-66 has a slope close to 2 in the terminal region, and its deviation from terminal zone slope of 2 can be attributed to polydispersed behavior of nylon-66.[39] In the low frequency region addition of clay led to an increase in value of storage modulus for all types of clays, however, this increase was more pronounced in the case of INa-MMT nanocomposite. As it can be seen from Figure 15 in the terminal region for the nanocomposites the plots have a slope less than 2 and the lowest slope belongs to INa-MMT nanocomposite. The differences in slopes may be ascribed to differences in extent of exfoliation. A larger extent of exfoliation will lead to more solid-like behavior due to increased number of clay-polymer interactions.[39] This is consistent with DMTA results in which the most height depression for tan δ occurred for INa-MMT nanocomposite indicating better dispersion of organoclay and larger contact area between the INa-MMT surface and nylon-66 chains.

CONCLUSIONS

Grafting reaction of alkyl silane through reaction with hydroxyl groups on the edge of clay was performed in dry toluene under sonication. In a separate method dry silane grafting was followed by mixing in water/ethanol solution, which led to better grafting of silane molecules regarding to TGA results that showed greater amount of weight loss in HS-MMT organoclay. FT-IR and XRD were also

used to confirm silane grafting process. IPC process improved the consistency of MMTs with nylon matrix as it was seen in XRD data and TEM images showing intercalated and exfoliated structures. Covalently bonded silane molecules enhanced thermal stability of nylon nanocomposite by 37°C according to observed T_{max} in TGA thermograms. DSC cooling scans revealed that interactive surfaces in silane modified clays that are capable of immobilizing chains can act as effective nucleating agent to facilitate nylon-66 crystallization. The largest contact area between the nanoclay surface and polymer chains and therefore, the largest amount of constrained region was observed for INa-MMT nanocomposite due to most height depression discerned in the tan δ peak in DMTA data. Rheology results also corroborated that INa-MMT-based nanocomposite has better dispersion of organoclay and larger contact area between the modified clay surface and nylon-66 matrix regarding to highest values for complex viscosity and strongest shear thinning behavior observed for this nanocomposite. It can be concluded that to improve thermal properties of nanocomposites i.e., thermal stability, silane grafted montmorillonites are efficiently practical. Additionally, as a particular method for modifying clay platelets, IPC process is utilized for synthesis of nylon-66 in the presence of nanoclay. Finally, in comparison with reported IPC processes in which nylon matrix of nanocomposites are prepared through polymerization of expensive monomers, the present method produces modified clay with very low content of nylon and much less monomer consumption.

References

1. Alexandre, M.; Dubois, P. Mater Sci Eng R 2000, 28, 1.
2. Pavlidou, S.; Papaspyrides, C. D. Prog Polym Sci 2008, 33, 1119.
3. Usuki, A.; Kawasumi, M.; Kojima, Y.; Okada, A.; Kurauchi, T.; Kamigaito, O. J Mater Res 1993, 8, 1174.
4. Usuki, A.; Kojima, Y.; Kawasumi, M.; Okada, A.; Fukushima, Y.; Kurauchi, T.; Kamigaito, O. J Mater Res 1993, 8, 1179.
5. Beyer, F. L.; Tan, N. C. B.; Dasgupta, A.; Galvin, M. E. Chem Mater 2002, 14, 2983.
6. Kim, G. M.; Lee, D. H.; Hoffmann, B.; Kressler, J.; Stöppelmann, G. Polymer 2001, 42, 1095.
7. Scaffaro, R.; Mistretta, M. C.; La Mantia, F. P. Polym Degrad Stab 2008, 93, 1267.
8. Xie, W.; Gao, Z.; Pan, W. P.; Hunter, D.; Singh, A.; Vaia, R. Chem Mater 2001, 13, 2979.
9. Herrera, N. N.; Letoffe, J. M.; Putaux, J. L.; David, L.; Bourgeat-Lami, E. Langmuir 2004, 20, 1564.
10. Isoda, K.; Kuroda, K.; Ogawa, M. Chem Mater 2000, 12, 1702.
11. Qian, Z.; Zhou, H.; Xu, X.; Ding, Y.; Zhang, S.; Yang, M. Polym Compos 2009, 30, 1234.
12. Song, K.; Sandi, G. Clays Clay Miner 2001, 49, 119.
13. He, H.; Duchet, J.; Galy, J.; Gerard, J. F. J Colloid Interface Sci 2005, 288, 171.
14. Shanmugharaj, A. M.; Rhee, K. Y.; Ryu, S. H. J Colloid Interface Sci 2006, 298, 854.
15. Herrera, N. N.; Letoffe, J. M.; Reymond, J. P.; Bourgeat-Lami, E. J Mater Chem 2005, 15, 863.
16. Shen, W.; He, H.; Zhu, J.; Yuan, P.; Frost, R. L. J Colloid Interface Sci 2007, 313, 268.
17. Dean, K. M.; Bateman, S. A.; Simons, R. Polymer 2007, 48, 2231.
18. Chow, W. S.; Neoh, S. S. J Appl Polym Sci 2009, 114, 3967.
19. Park, S. J.; Kim, B. J.; Seo, D. I.; Rhee, K. Y.; Lyu, Y. Y. Mater Sci Eng A 2009, 526, 74.
20. Sen, S. Polym Compos 2010, 31, 482.
21. Wan, C.; Bao, X.; Zhao, F.; Kandasubramanian, B.; Duggan, M. P. J Appl Polym Sci 2008, 110, 550.
22. Wang, K.; Wang, L.; Wu, J.; Chen, L.; He, C. Langmuir 2005, 21, 3613.
23. Xu, X.; Ding, Y.; Wang, F.; Wen, B.; Zhang, J.; Zhang, S.; Yang, M. Polym Compos 2010, 31, 825.
24. Mark, H. F.; Bikales, N. M.; Overberger, C. G.; Menges, G. Encyclopedia of Polymer Science and Engineering; Wiley: New York, 1988; Vol.11.
25. Kalkan, Z. S.; Goettler, L. A. Polym Eng Sci 2009, 49, 1491.
26. Kalkan, Z. S.; Goettler, L. A. Polym Eng Sci 2009, 49, 1825.
27. Tarameshlou, M.; Jafari, S.; Khonakdar, H. A.; Farmahini Farahani, M.; Ahmadian, S. Polym Compos 2007, 28, 733.
28. Worrall, W. E. Clays and Ceramic Raw Materials; Elsevier: New York, 1986.
29. Du, Y.; George, S. M. J Phys Chem C 2007, 111, 8509.
30. Chavarria, F.; Paul, D. R. Polymer 2004, 45, 8501.
31. Li, L.; Li, C. Y.; Ni, C.; Rong, L.; Hsiao, B. Polymer 2007, 48, 3452.
32. Barber, G. D.; Calhoun, B. H.; Moore, R. B. Polymer 2005, 46, 6706.
33. Dillon, D. R.; Tenneti, K. K.; Li, C. Y.; Ko, F. K.; Sics, I.; Hsiao, B. S. Polymer 2006, 47, 1678.
34. Zhang, Q. X.; Yu, Z. Z.; Yang, M.; Ma, J.; Mai, Y. W. J Polym Sci Part B: Polym Phys 2003, 41, 2861.
35. Masenelli-Varlot, K.; Reynaud, E.; Vigier, G.; Varlet, J. J Polym Sci Part B: Polym Phys 2002, 40, 272.
36. Yu, Z. Z.; Yan, C.; Yang, M.; Mai, Y. W. Polym Int 2004, 53, 1093.
37. Abdalla, M.; Dean, D.; Adibempe, D.; Nyairo, E.; Robinson, P.; Thompson, G. Polymer 2007, 48, 5662.
38. Zhang, X.; Loo, L. S. Macromolecules 2009, 42, 5196.
39. Fornes, T. D.; Yoon, P. J.; Keskkula, H.; Paul, D. R. Polymer 2001, 42, 09929.
40. Cho, J. W.; Paul, D. R. Polymer 2001, 42, 1083.